Applications of Mathematics

Cristian Lăzureanu; Camelia Petrişor; Ciprian Hedrea

On a deformed version of the two-disk dynamo system

Applications of Mathematics, Vol. 66 (2021), No. 3, 345–372

Persistent URL: http://dml.cz/dmlcz/148898

ON A DEFORMED VERSION OF THE TWO-DISK DYNAMO SYSTEM

Cristian Lăzureanu, Camelia Petrişor, Ciprian Hedrea, Timişoara

Received November 13, 2019. Published online March 5, 2021.

Abstract. We give some deformations of the Rikitake two-disk dynamo system. Particularly, we consider an integrable deformation of an integrable version of the Rikitake system. The deformed system is a three-dimensional Hamilton-Poisson system. We present two Lie-Poisson structures and also symplectic realizations. Furthermore, we give a prequantization result of one of the Poisson manifold. We study the stability of the equilibrium states and we prove the existence of periodic orbits. We analyze some properties of the energy-Casimir mapping $\mathcal{EC}$ associated to our system. In many cases the dynamical behavior of such systems is related with some geometric properties of the image of the energy-Casimir mapping. These connections were observed in the cases when the image of $\mathcal{EC}$ is a convex proper subset of $\mathbb{R}^2$. In order to point out new connections, we choose deformation functions such that $\mathrm{Im}(\mathcal{EC}) = \mathbb{R}^2$. Using the images of the equilibrium states through the energy-Casimir mapping we give parametric equations of some special orbits, namely heteroclinic orbits, split-heteroclinic orbits, and split-homoclinic orbits. Finally, we implement the mid-point rule to perform some numerical integrations of the considered system.

Keywords: integrable deformation; Hamilton-Poisson system; stability; energy-Casimir mapping; periodic orbit; heteroclinic orbit; mid-point rule

MSC 2020: 70H05, 70H06, 70H12, 70H14, 70K20, 70K44

1. Introduction

It is well-known that the shapes of the orbits of a three-dimensional Hamilton-Poisson system are given by the intersections of the level sets $H = h$ and $C = c$, where H is the Hamiltonian and C is a Casimir of the Poisson structure (see e.g. [16]). Denote by $\mathcal{S}$ the set of all pairs (h, c) for which the above mentioned intersection is nonempty. Consequently, every pair $(h, c) \in \mathcal{S}$ gives rise to an orbit. Moreover,

The work has been supported by research grants PCD-TC-2017 of Politehnica University Timişoara.

DOI: 10.21136/AM.2021.0303-19

h and c can be regarded as parameters, which leads to a kind of planar bifurcation diagram. Some curves of bifurcation that partition $\mathcal{S}$ into subsets in which a considered system has the same dynamics, are expected. Considering the energy-Casimir mapping $\mathcal{EC}$ corresponding to a three-dimensional Hamilton-Poisson system [38], the set $\mathcal{S}$ is the image of $\mathcal{EC}$ and the curves of bifurcation are given by the images of the equilibrium states through the energy-Casimir mapping (see also the curves of critical energy states [1]). Moreover, some connections between the dynamical properties of such systems and the image of the corresponding energy-Casimir mapping were reported (see also [26], [6]). In these works, the images of the energy-Casimir mappings of the considered systems are convex proper subsets of $\mathbb{R}^2$ and they provide a complete picture of the dynamics of the analyzed systems. Despite the fact that it was not proven, a general result, the presence of periodic orbits, as well as of homoclinic and heteroclinic orbits, can be predicted in these cases (see also [23]). On the other hand, in the case when the image of the energy-Casimir mapping is $\mathbb{R}^2$, the dynamics is more complex [39], [7] and the analysis of many systems is necessary.

In this paper, we analyze a three-dimensional Hamilton-Poisson system whose energy-Casimir mapping has the image $\mathbb{R}^2$. This system is related with the well-known Rikitake two-disk dynamo system, which is a simple mechanical system used to model the reversals of the Earth's magnetic field [14], [9]. The Rikitake system describes the currents of two coupled dynamo disks [37], [10]. It was widely analyzed. Among other topics, we mention: chaotic behavior [18], [40], dynamics [32], [44], [45], synchronization [43], [42], [20], and secure communication [34]. In [30], an integrable version of the Rikitake system was considered. We recall some topics related to this version: invariant algebraic surfaces [30], analytic and Darbouxian integrals [41], symplectic realization and some symmetries [27]. Furthermore, an extensive study from some standard and nonstandard Poisson geometry points of view was performed [38]. A fractional version of this system was studied in [19]. In [22], integrable deformations of an integrable version of the Rikitake system were obtained. By choosing particular deformation functions, one obtains new Hamilton-Poisson systems with various dynamical behavior.

The integrable deformations of integrable systems of ODEs were the subject of recent papers. If such a system is endowed with Lie-Poisson symmetries, a general method of construction of integrable deformations was proposed by considering Poisson-Lie groups as deformations of Lie-Poisson (co)algebras [4]. In [12] a family of integrable deformations of the Bogoyavlenskij-Itoh systems was constructed based on the fact that the Casimirs of a family of compatible Poisson structures for the undeformed systems provide a generating function for the integrals in involution of the deformed systems. In [13], [24], [28], integrable deformations of some three-dimensional Hamilton-Poisson systems were constructed. The new systems are

obtained by alteration of the constants of motion of the initial systems. The deformed systems are Hamilton-Poisson too, and they generalize initial systems. Furthermore, in [25] an integrable deformations method for three-dimensional systems of differential equations was introduced. Using this method, in this paper we give some deformations of the Rikitake system. Particularly, we consider deformation functions such that the image of the energy-Casimir mapping is $\mathbb{R}^2$. Our purpose is to study the new dynamics. On one hand, we try to establish how the dynamics is changed. On the other hand, we analyze which connections between the image of the energy-Casimir mapping and dynamical properties, that were established for the undeformed system, remain true. Moreover, we try to set out which kind of orbits can be predicted in such cases.

The paper is organized as follows. In Section 2, using the integrable deformations method for three-dimensional systems of differential equations [25], we construct some deformations of the Rikitake two-disk dynamo system. Section 3 deals with the study of a particular integrable deformation. Firstly, we present Hamilton-Poisson realizations and symplectic realizations of the considered system. We also give a prequantization result. Secondly, we study the stability of the equilibrium states of the system. Then we prove the existence of some periodic orbits. Moreover, in connection with the images of the equilibrium states through the energy-Casimir mapping, we point out some special orbits of the considered system, such as heteroclinic orbits, split-heteroclinic orbits, and split-homoclinic orbits. More precisely, for an arbitrary equilibrium state we consider the level sets of the Hamiltonian and Casimir functions at this point. Then we reduce the considered system from three degrees of freedom to one degree of freedom. Integrating the resulted differential equation we obtain a special solution of our system. In the last section we give a numerical integration of the considered system. There are several numerical integrators, but a geometric integrator, which preserves the constants of motion and the Poisson structure, eventually, is preferred. We implement the mid-point rule [3]. In our case this integrator is an almost Poisson integrator which preserves exactly the Hamiltonian and Casimir functions.

For details on Hamilton-Poisson mechanics, see, for example [29], [35] and references therein.

2. Deformations of the two-disk dynamo system

In this section we construct some deformations of the two-disk dynamo system. These deformations are obtained using the integrable deformations method for a three-dimensional system of differential equations [25]. We should mention here that in [17] deformations of the other version of the Rikitake system were considered.

Using some change of variables [10], [15] (also see [22]), a version of the Rikitake two-disk dynamo system is given by

$$\dot{x} = yz - rx + ay, \quad \dot{y} = xz - ax - ry, \quad \dot{z} = g - xy, \tag{2.1}$$

where $a \in \mathbb{R}$ and $g, r \geqslant 0$.

The above-mentioned method requires to identify a Hamilton-Poisson part of the considered system. More precisely, the system $\dot{\mathbf{x}} = \mathbf{g}(\mathbf{x})$ is a Hamilton-Poisson part of a three-dimensional system $\dot{\mathbf{x}} = \mathbf{g}(\mathbf{x}) + \mathbf{h}(\mathbf{x})$ if it has two functionally independent constants of motion. We identify more Hamilton-Poisson parts of system (2.1). For instance, we mention systems $\dot{x} = yz$, $\dot{y} = xz$, $\dot{z} = -xy$ and $\dot{x} = ay$, $\dot{y} = -ax$, $\dot{z} = -xy$. In the sequel we consider a widely investigated integrable version of system (2.1) given by the following equations (see, for example, [30]):

$$\dot{x} = yz + ay, \quad \dot{y} = xz - ax, \quad \dot{z} = -xy. \tag{2.2}$$

Integrable deformations of this system were given in [22], namely

$$\begin{aligned}
\dot{x} &= yz + ay + a\frac{\partial \alpha}{\partial y} + \frac{y}{2}\frac{\partial \alpha}{\partial z} - z\frac{\partial \beta}{\partial y} + \frac{y}{2}\frac{\partial \beta}{\partial z} + \frac{1}{2}\Big(\frac{\partial \alpha}{\partial y}\frac{\partial \beta}{\partial z} - \frac{\partial \alpha}{\partial z}\frac{\partial \beta}{\partial y}\Big),\\
\dot{y} &= xz - ax - a\frac{\partial \alpha}{\partial x} + \frac{x}{2}\frac{\partial \alpha}{\partial z} + z\frac{\partial \beta}{\partial x} - \frac{x}{2}\frac{\partial \beta}{\partial z} - \frac{1}{2}\Big(\frac{\partial \alpha}{\partial x}\frac{\partial \beta}{\partial z} - \frac{\partial \alpha}{\partial z}\frac{\partial \beta}{\partial x}\Big),\\
\dot{z} &= -xy - \frac{y}{2}\frac{\partial \alpha}{\partial x} - \frac{x}{2}\frac{\partial \alpha}{\partial y} - \frac{y}{2}\frac{\partial \beta}{\partial x} + \frac{x}{2}\frac{\partial \beta}{\partial y} + \frac{1}{2}\Big(\frac{\partial \alpha}{\partial x}\frac{\partial \beta}{\partial y} - \frac{\partial \alpha}{\partial y}\frac{\partial \beta}{\partial x}\Big),
\end{aligned} \tag{2.3}$$

where α and β are arbitrary differentiable functions on $\mathbb{R}^3$. It is obvious that if α and β vanish, then (2.3) reduces to (2.2).

We also recall that the functions C_1 and C_2 given by

$$\begin{aligned}
C_1(x, y, z) &= \frac{1}{2}x^2 + \frac{1}{2}y^2 + z^2 + \alpha(x, y, z),\\
C_2(x, y, z) &= \frac{1}{2}x^2 - \frac{1}{2}y^2 + 2az + \beta(x, y, z)
\end{aligned} \tag{2.4}$$

are constants of motion of system (2.3). Moreover, system (2.3) is bi-Hamiltonian, that is, it can be written in the form

$$\dot{x} = \{x, C_2\}_1 = \{x, C_1\}_2, \ \dot{y} = \{y, C_2\}_1 = \{y, C_1\}_2, \ \dot{z} = \{z, C_2\}_1 = \{z, C_1\}_2, \tag{2.5}$$

where the compatible Poisson brackets are given by

$$\{x, y\}_1 = -z - \frac{1}{2}\frac{\partial \alpha}{\partial z}, \quad \{x, z\}_1 = \frac{y}{2} + \frac{1}{2}\frac{\partial \alpha}{\partial y}, \quad \{y, z\}_1 = -\frac{x}{2} - \frac{1}{2}\frac{\partial \alpha}{\partial x} \tag{2.6}$$

and

$$\{x,y\}_2 = a + \frac{1}{2}\frac{\partial\beta}{\partial z}, \quad \{x,z\}_2 = \frac{y}{2} - \frac{1}{2}\frac{\partial\beta}{\partial y}, \quad \{y,z\}_2 = \frac{x}{2} + \frac{1}{2}\frac{\partial\beta}{\partial x}, \tag{2.7}$$

respectively [22].

Now, via the integrable deformation method [25], we obtain the following theorem.

Theorem 2.1. *Let α, β be arbitrary differentiable functions on $\mathbb{R}^3$. Then an integrable deformation of system* (2.1) *is given by the following system:*

$$\begin{aligned}
\dot{x} &= yz - rx + ay + a\frac{\partial\alpha}{\partial y} + \frac{y}{2}\frac{\partial\alpha}{\partial z} - z\frac{\partial\beta}{\partial y} + \frac{y}{2}\frac{\partial\beta}{\partial z} + \frac{1}{2}\Big(\frac{\partial\alpha}{\partial y}\frac{\partial\beta}{\partial z} - \frac{\partial\alpha}{\partial z}\frac{\partial\beta}{\partial y}\Big),\\
\dot{y} &= xz - ax - ry - a\frac{\partial\alpha}{\partial x} + \frac{x}{2}\frac{\partial\alpha}{\partial z} + z\frac{\partial\beta}{\partial x} - \frac{x}{2}\frac{\partial\beta}{\partial z} - \frac{1}{2}\Big(\frac{\partial\alpha}{\partial x}\frac{\partial\beta}{\partial z} - \frac{\partial\alpha}{\partial z}\frac{\partial\beta}{\partial x}\Big),\\
\dot{z} &= g - xy - \frac{y}{2}\frac{\partial\alpha}{\partial x} - \frac{x}{2}\frac{\partial\alpha}{\partial y} - \frac{y}{2}\frac{\partial\beta}{\partial x} + \frac{x}{2}\frac{\partial\beta}{\partial y} + \frac{1}{2}\Big(\frac{\partial\alpha}{\partial x}\frac{\partial\beta}{\partial y} - \frac{\partial\alpha}{\partial y}\frac{\partial\beta}{\partial x}\Big).
\end{aligned} \tag{2.8}$$

Note that the divergence of the flow of system (2.8) is $\nabla \cdot \tilde{\mathbf{f}} = -2r \leqslant 0$, which is in fact the divergence of the flow of two-disk dynamo system (2.1). Therefore, systems (2.1) and (2.8) are both dissipative or conservative.

In order to obtain an easier deformation, we consider the deformation functions $\alpha(x,y,z) = (b-1)z^2$ and $\beta(x,y,z) = 0$, where $b \in \mathbb{R}$ is a deformation parameter. In this case system (2.8) becomes

$$\dot{x} = byz - rx + ay, \quad \dot{y} = bxz - ax - ry, \quad \dot{z} = g - xy. \tag{2.9}$$

The main part of this paper, namely the study of an integrable case of the above system, is given in the next sections.

3. The study of a particular integrable deformation of the two-disk dynamo system

In this section we analyze a particular integrable deformation of the Rikitake system. More precisely, we present two Hamilton-Poisson realizations of the considered system and also symplectic realizations. Furthermore, we study the stability of the equilibrium states of the system and the existence of some periodic orbits. Finally, we give parametric representations of some special orbits, such as heteroclinic orbits or unbounded orbits, in connection with the image of the energy-Casimir mapping.

Consider $r = g = 0$. Then the deformed version of the two-disk dynamo given by (2.9) becomes the following particular integrable deformation of the Rikitake system:

$$\dot{x} = byz + ay, \quad \dot{y} = bxz - ax, \quad \dot{z} = -xy. \tag{3.1}$$

We notice that system (3.1) is an integrable version of the Rikitake system with the parametric control functions $u_1(x, y, z) = (b - 1)yz$ and $u_2(x, y, z) = (b - 1)xz$ about Ox and Oy axes, respectively, where b is the tunning parameter.

3.1. Lie-Poisson structures, symplectic realizations and geometric prequantization. The constants of motion of system (3.1) are given by (2.4), namely

$$C_1(x, y, z) = \frac{1}{2}x^2 + \frac{1}{2}y^2 + bz^2, \quad C_2(x, y, z) = \frac{1}{2}x^2 - \frac{1}{2}y^2 + 2az. \tag{3.2}$$

Considering C_1 as a Casimir function and C_2 the Hamiltonian, the corresponding Poisson bracket is given by (2.6)

$$\{x, y\}_1 = -bz, \quad \{x, z\}_1 = \frac{y}{2}, \quad \{y, z\}_1 = -\frac{x}{2}. \tag{3.3}$$

Following [22], we analogously obtain that this linear Poisson bracket corresponds to the Lie algebra $\mathfrak{so}(3)$,

$$\mathfrak{so}(3) = \left\{ X = \begin{bmatrix} 0 & -w & v \\ w & 0 & -u \\ -v & u & 0 \end{bmatrix} ; \ u, v, w \in \mathbb{R} \right\}.$$

We recall the proof [22]. Let $[\cdot, \cdot]_D$ be the nonstandard commutator on the space of skew-symmetric matrices $\mathfrak{so}(3)$ [8] given by $[X, Y]_D = XDY - YDX$, where $D = \mathrm{diag}(-\frac{1}{2}, -\frac{1}{2}, -b)$ is a diagonal matrix. A basis of $\mathfrak{so}(3)$ is given by $B_{\mathfrak{so}(3)} = \{f_1, f_2, f_3\}$, where

$$f_1 = \begin{bmatrix} 0 & 0 & 0 \\ 0 & 0 & -1 \\ 0 & 1 & 0 \end{bmatrix}, \quad f_2 = \begin{bmatrix} 0 & 0 & 1 \\ 0 & 0 & 0 \\ -1 & 0 & 0 \end{bmatrix}, \quad f_3 = \begin{bmatrix} 0 & -1 & 0 \\ 1 & 0 & 0 \\ 0 & 0 & 0 \end{bmatrix}.$$

We obtain $[f_1, f_2]_D = -bf_3$, $[f_1, f_3]_D = \frac{1}{2}f_2$, $[f_2, f_3]_D = -\frac{1}{2}f_1$. Therefore, the Lie-Poisson structure $\{\cdot, \cdot\}_1$ (3.3) is defined on $\mathfrak{so}(3)^* \simeq \mathbb{R}^3$. Taking into account (2.5), we obtain that system (3.1) has the Hamilton-Poisson realization $(\mathfrak{so}(3)^*, \{\cdot, \cdot\}_1, C_2)$.

Now, considering C_1 the Hamiltonian and C_2 the Casimir function, the second Poisson structure is given by (2.7), namely

$$\{x, y\}_2 = a, \quad \{x, z\}_2 = \frac{y}{2}, \quad \{y, z\}_2 = \frac{x}{2}. \tag{3.4}$$

This linear Poisson Bracket is in fact a modified Lie-Poisson bracket corresponding to Lie algebra $\mathfrak{e}(1,1)$,

$$\mathfrak{e}(1,1)=\left\{X=\begin{bmatrix}0&0&0\\ \alpha&0&\gamma\\ \beta&\gamma&0\end{bmatrix}\ ;\ \alpha,\beta,\gamma\in\mathbb{R}\right\}.$$

Indeed, considering the basis $B_{\mathfrak{e}(1,1)}=\{e_1,e_2,e_3\}$, where

$$e_1=\begin{bmatrix}0&0&0\\ 1&0&0\\ 0&0&0\end{bmatrix},\quad e_2=\begin{bmatrix}0&0&0\\ 0&0&0\\ -1&0&0\end{bmatrix},\quad e_3=\begin{bmatrix}0&0&0\\ 0&0&\frac{1}{2}\\ 0&\frac{1}{2}&0\end{bmatrix},$$

we get $[e_1,e_2]=0$, $[e_1,e_3]=\frac{1}{2}e_2$, $[e_2,e_3]=\frac{1}{2}e_1$.

Consider the bilinear form $\Theta\colon\ \mathfrak{e}(1,1)\times\mathfrak{e}(1,1)\to\mathbb{R}$ given by the matrix $(\Theta_{ij})_{1\leqslant i,j\leqslant 3}$, $\Theta_{12}=-\Theta_{21}=a$, and 0 otherwise. Then Θ is a symplectic cocycle of the Lie algebra $\mathfrak{e}(1,1)$. Because $\Theta(e_1,e_2)=a\neq 0=f([e_1,e_2])$, for every linear map $f,f\colon\ \mathfrak{e}(1,1)\to\mathbb{R}$, Θ is not a coboundary. Following [29], the modified Lie-Poisson structure $\{\cdot,\cdot\}_2$ of the dual space $\mathfrak{e}(1,1)^*\simeq\mathbb{R}^3$ associated with the symplectic cocycle Θ is defined. Therefore, system (3.1) has the Hamilton-Poisson realization $(\mathfrak{e}(1,1)^*,\{\cdot,\cdot\}_2,C_1)$. We mention that an interesting study of quadratic Hamilton-Poisson systems on $\mathfrak{e}(1,1)^*$ was performed in [5].

In the following we give symplectic realizations of the considered system.

Taking into account that the dynamics of a Hamilton-Poisson system is foliated by the symplectic leaves associated to the corresponding Poisson structure, it results that the restriction of the dynamics (3.1) to a regular leaf of each of the above Poisson structures is a Hamiltonian system. More precisely, we have:

Proposition 3.1. *Let $(\mathfrak{e}(1,1)^*\simeq\mathbb{R}^3,\{\cdot,\cdot\}_2,C_1)$ be a Hamilton-Poisson realization of system* (3.1)*, where the Poisson structure $\{\cdot,\cdot\}_2$ and the Hamiltonian C_1 are given by* (3.4) *and* (3.2)*, respectively. For every $c\in\mathbb{R}$, let $\mathcal{O}_c=C_2^{-1}(c)$ be the regular symplectic leaf of the Poisson structure $\{\cdot,\cdot\}_2$ with the Casimir function C_2 given by* (3.2)*. Then the restriction of system* (3.1) *to $\mathcal{O}_c$ is a Hamiltonian mechanical system, namely $(T^*\mathbb{R}\simeq\mathbb{R}^2,\omega,H)$, where the symplectic form is $\omega=adp\wedge dq$, and the Hamiltonian is given by*

$$H=\frac{1}{2}q^2+\frac{1}{2}p^2+\frac{b}{4a^2}\Big(c-\frac{1}{2}q^2+\frac{1}{2}p^2\Big)^2. \tag{3.5}$$

P r o o f. The Poisson bracket induced by ω is

$$\{f,g\}_\omega = a\Big(\frac{\partial f}{\partial q}\frac{\partial g}{\partial p} - \frac{\partial f}{\partial p}\frac{\partial q}{\partial p}\Big).$$

Hence, the dynamics of $(\mathbb{R}^2,\omega,H)$ is given by the equations

$$\begin{aligned}\dot q &= \{q,H\}_\omega = ap + \frac{b}{2a}\Big(c - \frac{1}{2}q^2 + \frac{1}{2}p^2\Big)p,\\ \dot p &= \{p,H\}_\omega = -aq + \frac{b}{2a}\Big(c - \frac{1}{2}q^2 + \frac{1}{2}p^2\Big)q.\end{aligned} \tag{3.6}$$

Let $c\in\mathbb{R}$. Then

$$C_2^{-1}(c) = \Big\{(x,y,z);\ z = \frac{1}{2a}\Big(c - \frac{1}{2}x^2 + \frac{1}{2}y^2\Big)\Big\}.$$

We define the immersion $\psi\colon\ \mathbb{R}^2\to\mathbb{R}^3$,

$$\psi(q,p) = (x,y,z) = \Big(q,p,\frac{1}{2a}\Big(c - \frac{1}{2}q^2 + \frac{1}{2}p^2\Big)\Big).$$

Then we obtain that equations (3.6) are mapped onto equations (3.1) and the canonical structure $\{\cdot,\cdot\}_\omega$ is mapped onto the Poisson structure $\{\cdot,\cdot\}_2$, which finishes the proof. □

The next result gives us another symplectic realization of the considered system.

Proposition 3.2. *The Hamilton-Poisson realization* $(\mathbb{R}^3,\{\cdot,\cdot\}_2,C_1)$ *of system* (3.1) *has a full symplectic realization* $(T^*\mathbb{R}^2\simeq\mathbb{R}^4,\omega,\widetilde H)$, *where*

$$\omega = a(dp_1\wedge dq_1 + dp_2\wedge dq_2) \quad \text{and} \quad \widetilde H = \frac{1}{2}q_1^2 + \frac{1}{2}p_1^2 + \frac{b}{4a^2}\Big(p_2 - \frac{1}{2}q_1^2 + \frac{1}{2}p_1^2\Big)^2.$$

P r o o f. The Hamilton's equations corresponding to $\widetilde H$ are:

$$\begin{cases}\dot q_1 = ap_1 + \dfrac{b}{2a}\Big(p_2 - \dfrac{1}{2}q_1^2 + \dfrac{1}{2}p_1^2\Big)p_1,\\ \dot q_2 = \dfrac{b}{2a}\Big(p_2 - \dfrac{1}{2}q_1^2 + \dfrac{1}{2}p_1^2\Big),\\ \dot p_1 = -aq_1 + \dfrac{b}{2a}\Big(p_2 - \dfrac{1}{2}q_1^2 + \dfrac{1}{2}p_1^2\Big)q_1,\\ \dot p_2 = 0.\end{cases} \tag{3.7}$$

We define the application $\varphi\colon\ \mathbb{R}^4\to\mathbb{R}^3$,

$$\varphi(q_1,q_2,p_1,p_2) = (x,y,z),\quad x = q_1,\quad y = p_1,\quad z = \frac{1}{2a}\Big(p_2 - \frac{1}{2}q_1^2 + \frac{1}{2}p_1^2\Big). \tag{3.8}$$

We obtain that φ is a submersion, equations (3.7) are mapped onto equations (3.1) and the Poisson structure $\{\cdot,\cdot\}_\omega$ induced by ω is mapped onto the Poisson structure $\{\cdot,\cdot\}_2$.

Therefore, $(\mathbb{R}^4,\omega,\widetilde{H})$ is a full symplectic realization of the Hamilton-Poisson mechanical system $(\mathbb{R}^3,\{\cdot,\cdot\}_2,C_1)$. □

Now, it is natural to ask whether system (3.7) is completely integrable in the Liouville's sense. The answer is affirmative.

Proposition 3.3. *The Hamiltonian mechanical system $(\mathbb{R}^4,\omega,\widetilde{H})$ considered above is completely integrable.*

P r o o f. System (3.7) has two differentiable first integrals $\widetilde{H}$ and $I=p_2$ that are in involution, $\{\widetilde{H},I\}_\omega=0$. Moreover, $d\widetilde{H}$ and dI are linearly independent on the dense open subset $\Omega=\{(q_1,q_2,p_1,p_2)\in\mathbb{R}^4;\ \operatorname{rank}J=2\}$ of $\mathbb{R}^4$, where J is the Jacobian matrix of $\widetilde{H}$ and I. The conclusion follows. □

In his classical book about quantum mechanics, Dirac has suggested that any classical Hamiltonian system can be "quantize" [11]. A prequantization of a symplectic manifold is a mapping that connects smooth functions with self-adjoint operators on a Hilbert space and satisfies the Dirac conditions. The existence of a prequantization is usually called the Dirac problem.

Following [21], the symplectic manifold $(T^*\mathbb{R}^2\simeq\mathbb{R}^4,\omega=d\theta)$, where $\theta=a(p_1\,dq_1+p_2\,dq_2)$, is quantizable from the geometric quantization point of view. The Hilbert representation space is $\mathcal{H}=L^2(\mathbb{R}^4,\mathbb{C})$, and the prequantum operator is given by δ^θ,

$$\delta^\theta\colon\ f\in C^\infty(T^*\mathbb{R}^2,\mathbb{R})\mapsto\delta^\theta_f\colon\ \mathcal{H}\to\mathcal{H},$$

where

$$\delta^\theta_f=-\mathrm{i}\hbar X_f-\theta(X_f)+f,$$

$\hbar$ is the Planck constant divided by 2π and

$$X_f=\sum_{k=1}^{2}a\Big(\frac{\partial f}{\partial p_k}\frac{\partial}{\partial q_k}-\frac{\partial f}{\partial q_k}\frac{\partial}{\partial p_k}\Big).$$

As we have seen, there is a connection between the Poisson manifold $(\mathbb{R}^3,\{\cdot,\cdot\}_2)$ and the symplectic manifold $(\mathbb{R}^4,\omega)$ considered above. In the following, we want to find out if the answer to Dirac's problem is affirmative in the case of this Poisson manifold, from Kostant's geometric prequantization point of view. This affirmative answer would mean the existence of a prequantization of the above Poisson manifold.

We can state the following prequantization result.

Proposition 3.4. *Let* $\mathcal{H} = L^2(\mathbb{R}^4, \mathbb{C})$ *and*

$$\delta\colon\ F \in C^\infty(\mathbb{R}^3, \mathbb{R}) \mapsto \delta_F, \quad \delta_F = \delta^\theta_{F\circ\varphi},$$

where φ *is given by* (3.8). *Then the pair* $(\mathcal{H}, \delta)$ *defines a prequantization of the Poisson manifold* $(\mathbb{R}^3, \{\cdot,\cdot\}_2)$.

P r o o f. Taking into account that the pair $(\mathcal{H}, \delta^\theta_f)$ given above defines a prequantization of $(T^*\mathbb{R}^2, \omega = d\theta)$, and the Poisson structure $\{\cdot,\cdot\}_\omega$ is mapped by application φ (3.8) onto the Poisson structure $\{\cdot,\cdot\}_2$, it is easy to see that Dirac's conditions (D_1)–(D_4) are all satisfied, where

(D_1) $\delta_{F+G} = \delta_F + \delta_G$ for all $F, G \in C^\infty(\mathbb{R}^3, \mathbb{R})$;
(D_2) $\delta_{\lambda F} = \lambda\delta_F$ for all $F \in C^\infty(\mathbb{R}^3, \mathbb{R})$, $\lambda \in \mathbb{R}$;
(D_3) $\delta_{1_{\mathbb{R}^3}} = \mathrm{Id}_{\mathcal{H}}$;
(D_4) $[\delta_F, \delta_G] = \mathrm{i}\hbar\delta_{\{F,G\}_2}$ for all $F, G \in C^\infty(\mathbb{R}^3, \mathbb{R})$

with $[\delta_F, \delta_G] = \delta_F \circ \delta_G - \delta_G \circ \delta_F$. □

3.2. Stability of equilibrium points. Let us continue with a discussion concerning the nonlinear stability of the equilibrium states of our system. As we explain later, in Subsection 3.4, we consider $b \in (-\infty, 0)$.

It is obvious that the equilibrium points of system (3.1) are given by

$$e_1^M = \Big(M, 0, \frac{a}{b}\Big), \quad e_2^M = \Big(0, M, -\frac{a}{b}\Big), \quad e_3^M = (0, 0, M), \tag{3.9}$$

where $M \in \mathbb{R}$.

Let A be the matrix of linear part of our system, that is

$$A = \begin{bmatrix} 0 & bz + a & by \\ bz - a & 0 & bx \\ -y & -x & 0 \end{bmatrix}.$$

The characteristic roots of $A(e_1^M)$ and $A(e_2^M)$ are given by $\lambda_1 = 0$, $\lambda_{2,3} = \pm\sqrt{-bM^2}$, hence we have obtained the following result.

Proposition 3.5. *For every* $M \in \mathbb{R}$, $M \neq 0$, *the equilibrium states* e_1^M *and* e_2^M (3.9) *of system* (3.1) *are unstable.*

The next result establishes the stability of the third equilibrium state.

Proposition 3.6. *Let e_3^M, $M \in \mathbb{R}$ (3.9) be an equilibrium state of system* (3.1).

(a) *If $|M| > |a/b|$, then e_3^M is an unstable equilibrium point.*
(b) *If $|M| < |a/b|$, then e_3^M is a nonlinearly stable equilibrium point.*

P r o o f. (a) The characteristic roots of $A(e_3^M)$ are given by $\lambda_1 = 0$, $\lambda_{2,3} = \pm\sqrt{b^2M^2 - a^2}$, and consequently, the equilibrium state e_3^M is unstable for each $M \in \mathbb{R}$ such that $M^2 > a^2/b^2$.

(b) We shall use Arnold's technique [2]. Consider the function

$$F_\lambda = C_1 + \lambda C_2 = \frac{1}{2}x^2 + \frac{1}{2}y^2 + bz^2 + \lambda\Big(\frac{1}{2}x^2 - \frac{1}{2}y^2 + 2az\Big).$$

We have:

(i) $\nabla F_\lambda(e_3^M) = 0$ if and only if $\lambda = -bM/a$;
(ii) Because

$$W := \ker[dC(e_3^M)] = \operatorname{Span}\left\{\begin{bmatrix}1\\0\\0\end{bmatrix}, \begin{bmatrix}0\\1\\0\end{bmatrix}\right\},$$

for all $v := (\alpha, \beta, 0) \in W$, $\alpha, \beta \in \mathbb{R}$ we get

$$v \cdot \nabla^2 F_{-bM/a}(e_3^M) \cdot v^\top = \Big(1 - \frac{bM}{a}\Big)\alpha^2 + \Big(1 + \frac{bM}{a}\Big)\beta^2,$$

which is positive definite in our case.

Therefore, via Arnold's stability test, the equilibrium state e_3^M is nonlinearly stable, as required. □

R e m a r k 3.7. We notice that $e_1^0 = e_3^{a/b}$ and $e_2^0 = e_3^{-a/b}$. In these cases the characteristic roots of the matrix A are $\lambda_1 = \lambda_2 = \lambda_3 = 0$. The stability of these equilibrium states remains an open problem.

3.3. Periodic orbits. In order to apply Moser's Theorem [33] regarding the existence of periodic orbits, we consider the restriction of our system to a regular coadjoint orbit of $\mathfrak{e}(1,1)^*$, obtained in Proposition 3.1, that contains a nonlinearly stable equilibrium point.

In the hypothesis of Proposition 3.1, the restriction of the nonlinearly stable equilibrium state $e_3^M = (0, 0, M)$, $|M| < |a/b|$ to $C_2^{-1}(c_2)$, where $c_2 = 2aM$, is the equilibrium state $(0, 0)$ of system (3.6). For the restricted dynamics, the existence of periodic orbits around this equilibrium point is proved in the next result.

Proposition 3.8. *Let $c_2 \in \mathbb{R}$ be such that $c_2^2 < 4a^4/b^2$. For sufficiently small $\varepsilon \in \mathbb{R}$, any integral surface*

$$\frac{1}{2}q^2 + \frac{1}{2}p^2 + \frac{b}{4a^2}\Big(c_2 - \frac{1}{2}q^2 + \frac{1}{2}p^2\Big)^2 - \frac{bc_2^2}{4a^2} = \varepsilon^2$$

contains at least one periodic solution of system (3.6) *whose period is close to the period of the corresponding linear system around* $(0,0)$, *namely*

$$2\pi\sqrt{\frac{4a^2}{4a^4 - b^2c_2^2}}.$$

P r o o f. The Hamiltonian H (3.5) is a constant of motion of system (3.6) with the property $dH(0,0) = 0$. We have successively:

(i) The matrix of linear part of our system at the point $(0,0)$ is

$$A(0,0) = \begin{bmatrix} 0 & a + \dfrac{bc_2}{2a} \\ -a + \dfrac{bc_2}{2a} & 0 \end{bmatrix}.$$

Therefore $A(0,0)$ is a nonsingular matrix.

(ii) The matrix $A(0,0)$ has a pair of pure complex eigenvalues

$$\lambda_{1,2} = \pm \mathrm{i}\sqrt{\frac{4a^4 - b^2c_2^2}{4a^2}}.$$

(iii)

$$d^2H(0,0) = \Big(1 - \frac{bc_2}{2a^2}\Big)dq^2 + \Big(1 + \frac{bc_2}{2a^2}\Big)dp^2$$

is positive definite.

Via Moser's Theorem, the conclusion follows. □

R e m a r k 3.9. The periodic orbits of the restricted dynamics (3.6) on the symplectic leaves are also periodic orbits for the unrestricted system (3.1) around the nonlinearly stable equilibrium states $(0,0,M)$.

3.4. The energy-Casimir mapping. Consider the Hamilton-Poisson realization $(\mathbb{R}^3, \{\cdot,\cdot\}_1, H)$ of system (3.1), where $H = C_2$ (see (3.2)) is the Hamiltonian and $C = C_1$ (see (3.2)) is a Casimir function of the Poisson structure $\{\cdot,\cdot\}_1$ (see (3.3)).

Using this geometric frame, the energy-Casimir mapping [38] associated to system (3.1) is defined by $\mathcal{EC}\colon \mathbb{R}^3 \to \mathbb{R}^2$,

$$\mathcal{EC}(x,y,z) = (H(x,y,z), C(x,y,z)) = \Big(\frac{1}{2}x^2 - \frac{1}{2}y^2 + 2az,\ \frac{1}{2}x^2 + \frac{1}{2}y^2 + bz^2\Big). \tag{3.10}$$

The image of the energy-Casimir mapping $\mathcal{EC}$ is the set

$$\begin{aligned}\mathrm{Im}(\mathcal{EC}) = \Big\{(h,c) \in \mathbb{R}^2;\ \exists\,(x,y,z) \in \mathbb{R}^3\colon\ &\frac{1}{2}x^2 - \frac{1}{2}y^2 + 2az = h,\\ &\frac{1}{2}x^2 + \frac{1}{2}y^2 + bz^2 = c\Big\}.\end{aligned} \tag{3.11}$$

In papers [38], [26], [6], some connections between the image of the energy-Casimir mapping and dynamical properties of the corresponding Hamilton-Poisson systems were reported. We notice that if $b \in [0,\infty)$, then we can show that for our system the set $\mathrm{Im}(\mathcal{EC})$ is a convex subset of $\mathbb{R}^2$, which looks similarly with those obtained in these works. Consequently, in the following we consider $b \in (-\infty, 0)$. We study the above-mentioned connections in this case.

The next result gives the set $\mathrm{Im}(\mathcal{EC})$.

Proposition 3.10. *Let $\mathcal{EC}$ be the energy-Casimir mapping* (3.10) *associated to system* (3.1). *If $b \in (-\infty, 0)$, then* $\mathrm{Im}(\mathcal{EC}) = \mathbb{R}^2$.

P r o o f. Using algebraic computations, by (3.11) we get the conclusion. □

Taking into account that the equilibrium states of system (3.1) are the critical points of the energy-Casimir mapping, their images through $\mathcal{EC}$ lead to a partition of $\mathrm{Im}(\mathcal{EC})$ (see Figure 1). We have:

$$\begin{aligned}
\Sigma_1^u &:= \mathcal{EC}(e_1^M) = \Big\{(h,c);\ c = h - \frac{a^2}{b},\ h > \frac{2a^2}{b}\Big\},\\
\Sigma_2^u &:= \mathcal{EC}(e_2^M) = \Big\{(h,c);\ c = -h - \frac{a^2}{b},\ h < -\frac{2a^2}{b}\Big\},\\
\Sigma_3^s &:= \mathcal{EC}(e_3^{M,s}) = \Big\{(h,c);\ c = \frac{b}{4a^2}h^2,\ |h| < -\frac{2a^2}{b}\Big\},\\
\Sigma_3^u &:= \mathcal{EC}(e_3^{M,u}) = \Big\{(h,c);\ c = \frac{b}{4a^2}h^2,\ |h| > -\frac{2a^2}{b}\Big\},
\end{aligned} \tag{3.12}$$

where the superscripts u and s stand for unstable and stable, respectively.

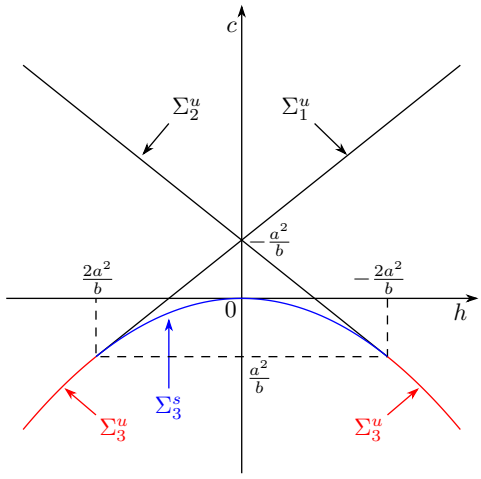

Figure 1. The images of the equilibrium states through the energy-Casimir mapping ($a = 1$, $b = -1$).

R e m a r k 3.11. The intersections of the curves that represent the images of the equilibrium states through the energy-Casimir mapping (see Figure 1) give three bifurcation points, namely

$$\Sigma_1^u \cap \Sigma_2^u = \Big\{\Big(0, -\frac{a^2}{b}\Big)\Big\}, \quad \mathcal{EC}\Big(0, 0, \frac{a}{b}\Big) = \Big\{\Big(\frac{2a^2}{b}, \frac{a^2}{b}\Big)\Big\}$$

and

$$\mathcal{EC}\Big(0, 0, -\frac{a}{b}\Big) = \Big\{\Big(-\frac{2a^2}{b}, \frac{a^2}{b}\Big)\Big\}.$$

We use these points to discuss some special orbits of the considered dynamics.

3.5. Types of special orbits of the considered dynamics. The fiber of the energy-Casimir mapping $\mathcal{EC}$ corresponding to an element $(h, c) \in \mathrm{Im}(\mathcal{EC})$ is the set

$$\mathcal{F}_{(h,c)} = \{(x, y, z) \in \mathbb{R}^3;\ \mathcal{EC}(x, y, z) = (h, c)\}. \tag{3.13}$$

For a pair (h, c), the implicit equation of the corresponding fiber is given by

$$\mathcal{F}_{(h,c)}\colon \begin{cases} H(x, y, z) = h, \\ C(x, y, z) = c. \end{cases} \tag{3.14}$$

Because the dynamics of a Hamilton-Poisson system takes place at the intersection of the level sets H = constant, C = constant, the above fiber gives the implicit representation of an orbit of the considered system.

Let (x_e, y_e, z_e) be an arbitrary critical point of $\mathcal{EC}$ and let $\mathcal{EC}(x_e, y_e, z_e) = (h_e, c_e)$. Then we say that the fiber $\mathcal{F}_{(h_e,c_e)}$ contains a special orbit of the considered system. Following [38], using the implicit equation of $\mathcal{F}_{(h_e,c_e)}$, it is possible to reduce the considered system from three degrees of freedom to one degree of freedom. If the resulted differential equation can be explicitly integrated, then the equations of a special orbit are obtained. In our case, the pair (h_e, c_e) belongs to the one of the sets Σ_1^u, Σ_2^u, Σ_3^u, or Σ_3^s. Particularly, (h_e, c_e) can be

$$\mathcal{EC}\Big(0, 0, \frac{a}{b}\Big) = \Big\{\Big(\frac{2a^2}{b}, \frac{a^2}{b}\Big)\Big\}$$

or

$$\mathcal{EC}\Big(0, 0, -\frac{a}{b}\Big) = \Big\{\Big(-\frac{2a^2}{b}, \frac{a^2}{b}\Big)\Big\}.$$

We start our discussion with the pair $(h, c) \in \Sigma_1^u \cap \Sigma_2^u$, that is $(0, -a^2/b)$. Imposing the condition $\mathcal{EC}(x, y, z) = (0, -a^2/b)$, we get

$$x = \pm\sqrt{-b}\Big(z + \frac{a}{b}\Big), \quad y = \pm\sqrt{-b}\Big(z - \frac{a}{b}\Big). \tag{3.15}$$

Then the last equation of system (3.1) becomes

$$\frac{\mathrm{d}z}{\mathrm{d}t} = \pm b\Big(z^2 - \frac{a^2}{b^2}\Big).$$

Integrating this equation we obtain

$$\Big|\frac{z + |a|/b}{z - |a|/b}\Big| = \mathrm{e}^{\pm 2|a|t + k}, \quad k \in \mathbb{R}.$$

Then we consider

$$z_1(t) = \frac{a}{b}\,\frac{\mathrm{e}^{p(t)} - 1}{\mathrm{e}^{p(t} + 1}, \quad z_2(t) = \frac{a}{b}\,\frac{\mathrm{e}^{p(t)} + 1}{\mathrm{e}^{p(t)} - 1}, \tag{3.16}$$

where

$$p(t) = 2|a|t + k. \tag{3.17}$$

Using (3.15), we denote

$$x_1(t) = \frac{2a}{\sqrt{-b}}\,\frac{\mathrm{e}^{p}(t)}{\mathrm{e}^{p(t)} + 1}, \quad x_2(t) = \frac{-2a}{\sqrt{-b}}\,\frac{\mathrm{e}^{p}(t)}{\mathrm{e}^{p(t)} - 1}, \tag{3.18}$$

$$y_1(t) = \frac{2a}{\sqrt{-b}}\,\frac{1}{\mathrm{e}^{p(t)} + 1}, \quad y_2(t) = \frac{2a}{\sqrt{-b}}\,\frac{1}{\mathrm{e}^{p(t)} - 1}, \tag{3.19}$$

respectively.

We recall that a heteroclinic orbit $\mathcal{HE}\colon \mathbb{R} \to \mathbb{R}^3$ is a solution $(x(t), y(t), z(t))$ of the considered system that connects two unstable equilibrium points p_1 and p_2 of the system, that is, $\mathcal{HE}(t) := (x(t), y(t), z(t))$ and $\mathcal{HE}(t) \to p_1$ as $t \to -\infty$, $\mathcal{HE}(t) \to p_2$ as $t \to \infty$. Also, a homoclinic orbit $\mathcal{H}\colon \mathbb{R} \to \mathbb{R}^3$ is a solution $(x(t), y(t), z(t))$ of the considered system which joins an unstable equilibrium point p to itself ($p_1 = p_2 = p$), that is, $\mathcal{H}(t) := (x(t), y(t), z(t))$ and $\mathcal{H}(t) \to p$ as $t \to \pm\infty$.

By analogy, if $(x(t), y(t), z(t))$, $t \in (-\infty, s_1)$ is a solution of the considered system such that $(x(t), y(t), z(t)) \to p_1$ as $t \to -\infty$, and also $(x(t), y(t), z(t))$, $t \in (s_2, \infty)$ is a solution of the considered system such that $(x(t), y(t), z(t)) \to p_2$ as $t \to \infty$, where $s_1 < s_2$, we say that $\mathcal{SHE}\colon (-\infty, s_1) \cup (s_2, \infty) \to \mathbb{R}^3$, $\mathcal{SHE}(t) := (x(t), y(t), z(t))$ is a "split-heteroclinic" orbit. Furthermore, if $p_1 = p_2$, the above split-heteroclinic orbit becomes a "split-homoclinic" orbit.

Observing that system (3.1) is invariant to the transformation $(x, y, z) \to (-x, -y, z)$, we have proved the following result.

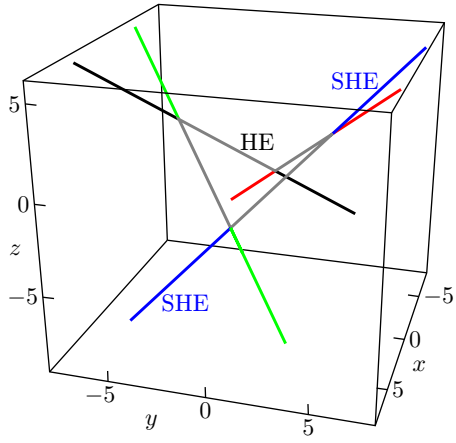

Figure 2. The fiber $\mathcal{F}_{(h,c)}$, $(h, c) = (0, -a^2/b)$ $(a = 2,\ b = -1)$.

Proposition 3.12. *Let $(h, c) = (0, -a^2/b) \in \Sigma_1^u \cap \Sigma_2^u$ and let us consider the functions given by* (3.16), (3.17), (3.18), (3.19). *Then the fiber $\mathcal{F}_{(h,c)}$ contains the following curves (see Figure* 2*):*

(i) *a heteroclinic orbit $\mathcal{HE}_1 := (x_1, y_1, z_1)\colon \mathbb{R} \to \mathbb{R}^3$ that connects the unstable equilibrium points $e_1^{2a/\sqrt{-b}} = (2a/\sqrt{-b}, 0, a/b)$ and $e_2^{2a/\sqrt{-b}} = (0, 2a/\sqrt{-b}, -a/b)$;*

(ii) *a heteroclinic orbit $\mathcal{HE}_2 := (-x_1, -y_1, z_1)\colon \mathbb{R} \to \mathbb{R}^3$ that connects the unstable equilibrium points $e_1^{-2a/\sqrt{-b}}$ and $e_2^{-2a/\sqrt{-b}}$;*

(iii) *a heteroclinic orbit $\mathcal{HE}_3 := (-y_1, x_1, -z_1)\colon \mathbb{R} \to \mathbb{R}^3$ that connects the unstable equilibrium points $e_1^{-2a/\sqrt{-b}}$ and $e_2^{2a/\sqrt{-b}}$;*

(iv) *a heteroclinic orbit* $\mathcal{HE}_4 := (y_1, -x_1, -z_1)\colon\ \mathbb{R} \to \mathbb{R}^3$ *that connects the unstable equilibrium points* $e_1^{2a/\sqrt{-b}}$ *and* $e_2^{-2a/\sqrt{-b}}$;

(v) *four split-heteroclinic orbits* $\mathcal{SHE}_i\colon\ \mathbb{R} \setminus \{-k/(2|a|)\} \to \mathbb{R}^3$, $i \in \{1,2,3,4\}$, *where* $\mathcal{SHE}_1 := (x_2, y_2, z_2)$, $\mathcal{SHE}_2 := (-x_2, -y_2, z_2)$, $\mathcal{SHE}_3 := (-y_2, x_2, -z_2)$, $\mathcal{SHE}_4 := (y_2, -x_2, -z_2)$.

In the same manner we obtain other special orbits.

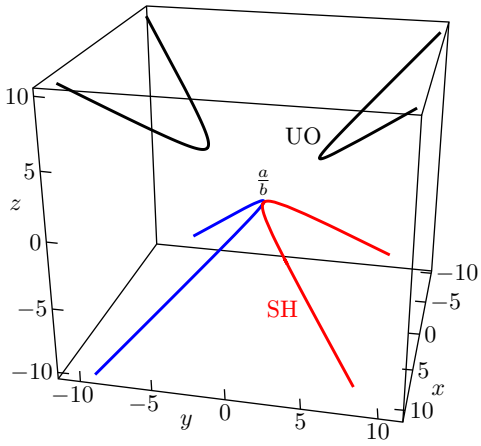

Figure 3. The fiber $\mathcal{F}_{(h,c)}$, $(h,c) = (2a^2/b, a^2/b)$ $(a = 1,\ b = -1)$.

Proposition 3.13. *Let* $k \in \mathbb{R}$. *Denote*

$$x(t) = \frac{-8a^2\sqrt{-b}(bt+k)}{4a^2b^2t^2 + 8a^2bkt + 4a^2k^2 - b^2}, \quad y(t) = \frac{4ab\sqrt{-b}}{4a^2b^2t^2 + 8a^2bkt + 4a^2k^2 - b^2},$$
$$z(t) = \frac{a(4a^2b^2t^2 + 8a^2bkt + 4a^2k^2 + 3b^2)}{b(4a^2b^2t^2 + 8a^2bkt + 4a^2k^2 - b^2)}.$$

(a) *Let* $(h,c) = (2a^2/b, a^2/b) = \mathcal{EC}(0,0,a/b)$. *Then the fiber* $\mathcal{F}_{(h,c)}$ *contains the following curves (see Figure* 3*):*

(i) *two unbounded orbits*

$$\mathcal{UO}^{\pm} := (\pm x, \pm y, z)\colon\ \Big(-\frac{k}{b} - \frac{1}{2|a|}, -\frac{k}{b} + \frac{1}{2|a|}\Big) \to \mathbb{R}^3;$$

(ii) *two split-homoclinic orbits*

$$\mathcal{SH}^{\pm}\colon\ \Big(-\infty, -\frac{k}{b} - \frac{1}{2|a|}\Big) \cup \Big(-\frac{k}{b} + \frac{1}{2|a|}, \infty\Big) \to \mathbb{R}^3, \quad \mathcal{SH}^{\pm} := (\pm x, \pm y, z),$$

which tend to a/b *as* $t \to \pm\infty$.

(b) *Let* $(h,c) = (-2a^2/b, a^2/b) = \mathcal{EC}(0,0,-a/b)$. *Then the fiber* $\mathcal{F}_{(h,c)}$ *contains the following curves:*

(i) *two unbounded orbits*

$$\mathcal{UO}^{\pm} := (\pm y, \mp x, -z)\colon \Big(-\frac{k}{b} - \frac{1}{2|a|}, -\frac{k}{b} + \frac{1}{2|a|}\Big) \to \mathbb{R}^3;$$

(ii) *two split-homoclinic orbits*

$$\mathcal{SH}^{\pm}\colon \Big(-\infty, -\frac{k}{b} - \frac{1}{2|a|}\Big) \cup \Big(-\frac{k}{b} + \frac{1}{2|a|}, \infty\Big) \to \mathbb{R}^3, \quad \mathcal{SH}^{\pm} := (\pm y, \mp x, -z),$$

which tends to $-a/b$ *as* $t \to \pm\infty$.

Proposition 3.14. *Let* $a > 0$ *and* $(h,c) \in \Sigma_1^u$. *Denote*

$$\begin{aligned}
x_1(t) &= -\sqrt{-b}\sqrt{4a^2 - 2bh}\,\frac{\mathrm{e}^{2p(t)} - 2bh}{b(\mathrm{e}^{2p(t)} + 4a\mathrm{e}^{p(t)} + 2bh)},\\
y_1(t) &= -2\sqrt{-b}\,\frac{(4a^2 - 2bh)\mathrm{e}^{p(t)}}{b(\mathrm{e}^{2p(t)} + 4a\mathrm{e}^{p(t)} + 2bh)},\\
z_1(t) &= \frac{a\mathrm{e}^{2p(t)} - 4a^2\mathrm{e}^{p(t)} + 4b\mathrm{e}^{p(t)}h + 2abh}{b(\mathrm{e}^{2p(t)} + 4a\mathrm{e}^{p(t)} + 2bh)},\\
x_2(t) &= \sqrt{-b}\sqrt{4a^2 - 2bh}\,\frac{\mathrm{e}^{2p(t)} - 2bh}{b(\mathrm{e}^{2p(t)} - 4a\mathrm{e}^{p(t)} + 2bh)},\\
y_2(t) &= -2\sqrt{-b}\,\frac{(4a^2 - 2bh)\mathrm{e}^{p(t)}}{b(\mathrm{e}^{2p(t)} - 4a\mathrm{e}^{p(t)} + 2bh)},\\
z_2(t) &= \frac{a\mathrm{e}^{2p(t)} + 4a^2\mathrm{e}^{p(t)} - 4bh\mathrm{e}^{p(t)} + 2abh}{b(\mathrm{e}^{2p(t)} - 4a\mathrm{e}^{p(t)} + 2bh)},
\end{aligned}$$

where $p(t) = \sqrt{4a^2 - 2bh}(t + k)$ *and* $k \in \mathbb{R}$.

(a) *If* $h \in (2a^2/b, 0]$, *then the fiber* $\mathcal{F}_{(h,c)}$ *contains the following curves (see Figure* 4*):*

(i) *two unbounded orbits* $\mathcal{UO}^{\pm} := (\pm x_2, \pm y_2, z_2)$ *defined on*

$$\Big(-k + \frac{\ln(2a - \sqrt{4a^2 - 2bh})}{\sqrt{4a^2 - 2bh}}, -k + \frac{\ln(2a + \sqrt{4a^2 - 2bh})}{\sqrt{4a^2 - 2bh}}\Big);$$

(ii) *a pair of heteroclinic orbits* $\mathcal{HE}^{\pm} := (\pm x_1, \pm y_1, z_1)\colon \mathbb{R} \to \mathbb{R}^3$ *that connects the unstable equilibrium points* e_1^M *and* e_1^{-M}, $M = \sqrt{2h - 4a^2/b}$;

(iii) *two split-heteroclinic orbits*

$$\mathcal{SHE}^{\pm}\colon \Big(-\infty, -k + \frac{\ln(2a - \sqrt{4a^2 - 2bh})}{\sqrt{4a^2 - 2bh}}\Big) \cup \Big(-k + \frac{\ln(2a + \sqrt{4a^2 - 2bh})}{\sqrt{4a^2 - 2bh}}, \infty\Big) \to \mathbb{R}^3,$$

where $\mathcal{SHE}^{\pm} := (\pm x_2, \pm y_2, z_2)$.

(b) *If $h \in (0,\infty)$, then the fiber $\mathcal{F}_{(h,c)}$ contains four split-heteroclinic orbits (see Figure 5), namely*

$$\mathcal{SHE}_1^{\pm}\colon\ \mathbb{R}\setminus\left\{-k+\frac{\ln(-2a+\sqrt{4a^2-2bh})}{\sqrt{4a^2-2bh}}\right\}\to\mathbb{R}^3,\quad \text{where } \mathcal{SHE}_1^{\pm}:=(\pm x_1,\pm y_1,z_1),$$

$$\mathcal{SHE}_2^{\pm}\colon\ \mathbb{R}\setminus\left\{-k+\frac{\ln(2a+\sqrt{4a^2-2bh})}{\sqrt{4a^2-2bh}}\right\}\to\mathbb{R}^3,\quad \text{where } \mathcal{SHE}_2^{\pm}:=(\pm x_2,\pm y_2,z_2).$$

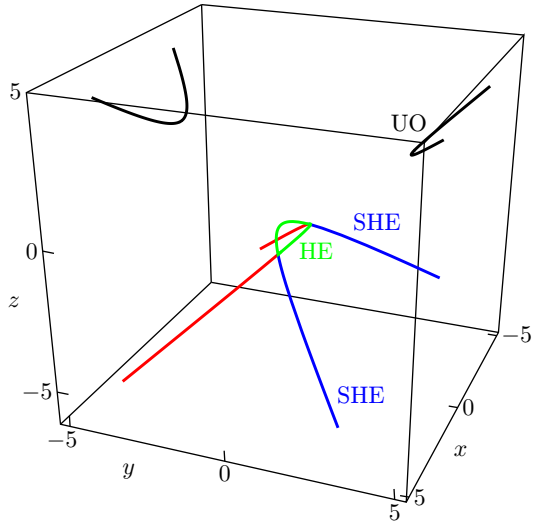

Figure 4. The fiber $\mathcal{F}_{(h,c)}$, $(h,c)\in\Sigma_1^u$, $h\in(2a^2/b,0]$ $(a=1,\ b=-1)$.

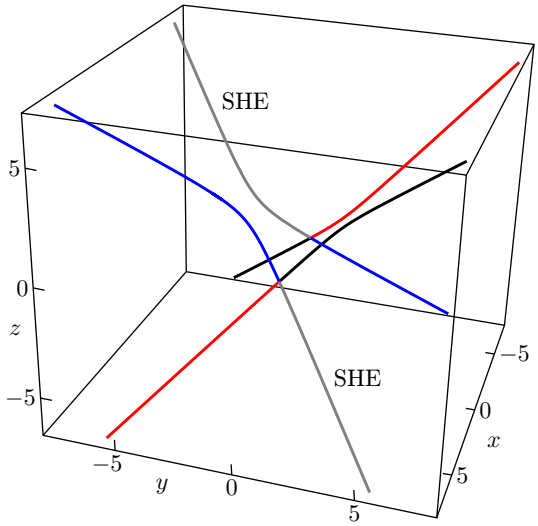

Figure 5. The fiber $\mathcal{F}_{(h,c)}$, $(h,c)\in\Sigma_1^u$, $h\in(0,\infty)$ $(a=1,\ b=-1)$.

R e m a r k 3.15. For $a < 0$ and $(h, c) \in \Sigma_1^u$ we have obtained similar curves to that ones from Proposition 3.14. Moreover, if $(h, c) \in \Sigma_2^u$, then the fiber $\mathcal{F}_{(h,c)}$ contains the same types of special orbits as those obtained in Proposition 3.14.

R e m a r k 3.16. Other special orbits correspond to an arbitrary pair $(h, c) \in \Sigma_3^u \cup \Sigma_3^s$. In these cases we have obtained the same types of orbits. More precisely, if $(h, c) \in \Sigma_3^u$, then the special orbits are two unbounded orbits and two split-homoclinic orbits (see Figure 3). Furthermore, if $(h, c) \in \Sigma_3^s$, then the fiber $\mathcal{F}_{(h,c)}$ contains eight unbounded orbits (Figure 6), but the difference to the above unbounded orbits is given by their parametric representations. We denote

$$
\begin{aligned}
x_1(t) &= \frac{-\sqrt{-b}(2a^2+bh)\sqrt{(4a^2-2bh)(1+\sin p(t))}}{b(bh+2a^2\sin p(t))},\\
y_1(t) &= \frac{\sqrt{-b}(2a^2-bh)\sqrt{(4a^2+2bh)(1-\sin p(t))}}{b(bh+2a^2\sin p(t))},\\
z_1(t) &= \frac{h}{2a}+\frac{4a^4-b^2h^2}{ab^2h+2a^3b\sin p(t)},\\
x_2(t) &= \frac{\sqrt{-b}(2a^2+bh)\sqrt{(4a^2-2bh)(1-\sin p(t))}}{b(bh-2a^2\sin p(t))},\\
y_2(t) &= \frac{\sqrt{-b}(2a^2-bh)\sqrt{(4a^2+2bh)(1+\sin p(t))}}{b(bh-2a^2\sin p(t))},\\
z_2(t) &= \frac{h}{2a}+\frac{4a^4-b^2h^2}{ab^2h-2a^3b\sin p(t)},
\end{aligned}
$$

where

$$
p(t) = \frac{\sqrt{4a^4-b^2h^2}}{|a|}(t+k) \quad \text{and} \quad k \in \mathbb{R}.
$$

Then, for example, in the case $a > 0$ and $h < 0$, let

$$
\begin{aligned}
t_1 &= -\frac{|a|}{\sqrt{4a^4-b^2h^2}}\arcsin\frac{bh}{2a^2}-k,\\
t_2 &= \frac{|a|}{\sqrt{4a^4-b^2h^2}}\Big(\pi+\arcsin\frac{bh}{2a^2}\Big)-k,\\
t_3 &= \frac{|a|}{\sqrt{4a^4-b^2h^2}}\arcsin\frac{bh}{2a^2}-k,\\
t_4 &= \frac{|a|}{\sqrt{4a^4-b^2h^2}}\Big(\pi-\arcsin\frac{bh}{2a^2}\Big)-k.
\end{aligned}
$$

The above-mentioned unbounded orbits are given by

$$
\begin{aligned}
&(\pm x_1, \pm y_1, z_1)\colon\ (t_1, t_2) \to \mathbb{R}, \quad (\pm x_1, \pm y_1, z_1)\colon\ (t_2, t_1+2\pi) \to \mathbb{R},\\
&(\pm x_2, \pm y_2, z_2)\colon\ (t_3, t_4) \to \mathbb{R}, \quad (\pm x_2, \pm y_2, z_2)\colon\ (t_4, t_3+2\pi) \to \mathbb{R}.
\end{aligned}
$$

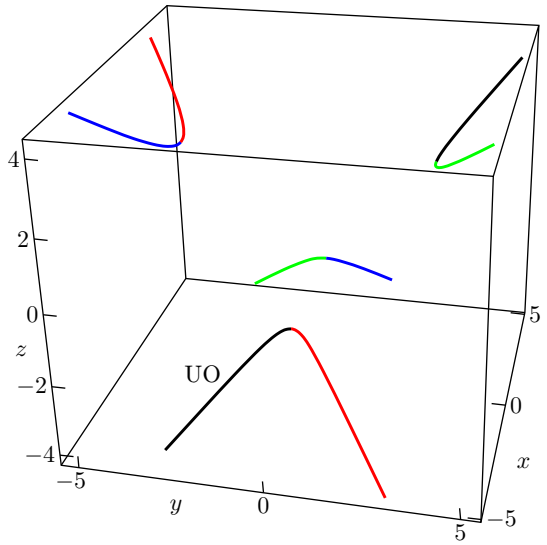

Figure 6. The fiber $\mathcal{F}_{(h,c)}$, $(h,c) \in \Sigma_3^s$ $(a=1,\, b=-1)$.

R e m a r k 3.17. In the case when $\mathrm{Im}(\mathcal{EC})$ is a convex proper subset of $\mathbb{R}^2$ and (h,c) belongs to the interior of this set, we expect the following. If (h,c) belongs to a line, then the fiber $\mathcal{F}_{(h,c)}$ contains one or more heteroclinic orbits. Also, if (h,c) belongs to a parabola, then the fiber $\mathcal{F}_{(h,c)}$ contains one or more homoclinic orbits. Otherwise, the fiber $\mathcal{F}_{(h,c)}$ contains periodic orbits (see [6], [26], [38]). In our case, instead of homoclinic orbits, we have obtained split-homoclinic orbits and unbounded orbits. Also, besides heteroclinic orbits we have obtained split-heteroclinic orbits and unbounded orbits.

In Subsection 3.3 we have proven the existence of the periodic orbits around the stable equilibrium states $(0,0,M)$. Using Proposition 3.1 and Proposition 3.8, we obtain the next result.

R e m a r k 3.18. The fiber $\mathcal{F}_{(h,c)}$ contains a periodic orbit if

$$|h| < -\frac{2a^2}{b}, \quad c > \frac{b}{4a^2}h^2, \quad c < h - \frac{a^2}{b}, \quad c < -h - \frac{a^2}{b},$$

or in other words, if (h,c) belongs to the bounded set situated between the curves Σ_1^u, Σ_2^u, Σ_3^s (see Figure 1).

4. Numerical integration

In the previous section we have explicitly obtained parametric equations of some special orbits of the considered system. This fact was possible because of particular forms of the fibers $\mathcal{F}_{(h,c)}$, given by $(h,c) = \mathcal{EC}(x_e, y_e, z_e)$. These orbits and the others can be obtained by numerical integration. As we already have proven there are periodic orbits in the dynamics of the considered system, but their equations are not obtained in the previous section. We point out such orbits by numerical integration.

Taking into account the geometric frame of the considered system, a numerical integrator which preserves as much as possible from its Poisson geometry, that is Poisson structure, symplectic leaves, Casimirs, and even the energy, it would be interesting. If the Hamiltonian function is separable, an explicit numerical integrator which preserves the Poisson structure, symplectic leaves, and Casimirs is given by the so-called Lie-Trotter algorithm (see, for example, [31], [36]). This algorithm does not preserve the Hamiltonian. Consequently, a numerical solution does not belong to the intersection of the level sets $H(x,y,z) = h$, $C(x,y,z) = c$.

In this section we apply the mid-point rule (see [3] and references therein) to system (3.1). Under some conditions this integrator has some of the above-mentioned properties.

We recall that for a Hamilton-Poisson system $\dot{\mathbf{x}} = \Pi(\mathbf{x})\nabla H(\mathbf{x}), \mathbf{x} = (x,y,z)^\top$, where Π is a Poisson structure and H the Hamiltonian function, the mid-point rule is given by the following implicit recursion [3]:

$$\frac{\mathbf{x}_{k+1} - \mathbf{x}_k}{\Delta t} = \Pi\Big(\frac{\mathbf{x}_k + \mathbf{x}_{k+1}}{2}\Big)\nabla H\Big(\frac{\mathbf{x}_k + \mathbf{x}_{k+1}}{2}\Big),$$

where Δt is the time-step. "If $\Pi(\mathbf{x})$ is linear in $\mathbf{x}$, then the mid-point rule is an almost Poisson integrator, that is, it preserves the Poisson structure up to the second order" [3]. Furthermore, "the mid-point rule preserves exactly any conserved quantity having only linear and quadratic terms" [3].

In the frame of the Hamilton-Poisson realization considered in 3.4, the integrator for system (3.1) has the form

$$\begin{aligned}
\frac{x_{k+1} - x_k}{\Delta t} &= a\frac{y_k + y_{k+1}}{2} + b\frac{(y_k + y_{k+1})(z_k + z_{k+1})}{4},\\
\frac{y_{k+1} - y_k}{\Delta t} &= -a\frac{x_k + x_{k+1}}{2} + b\frac{(x_k + x_{k+1})(z_k + z_{k+1})}{4},\\
\frac{z_{k+1} - z_k}{\Delta t} &= -\frac{(x_k + x_{k+1})(y_k + y_{k+1})}{4}.
\end{aligned} \tag{4.1}$$

R e m a r k 4.1. Because the Poisson bracket (3.3) is linear, the mid-point rule of system (3.1) given by (4.1) is an almost Poisson integrator. Moreover, the Hamiltonian function H and the Casimir C (3.10) are preserved by this integrator. Therefore numerical solutions belong to the intersection of the level sets $H(x,y,z)=h$, $C(x,y,z)=c$.

In the following we explain how the mid-point rule for the considered system works.

Consider a pair $(h,c)\in \mathrm{Im}(\mathcal{EC})$. If we focus on orbits which are not explicitly obtained in the previous section, then $(h,c)\neq \mathcal{EC}(x_e,y_e,z_e)$ for all equilibrium states (x_e,y_e,z_e) of system (3.1). Such orbits belong to the intersection of the level sets $H(x,y,z)=h$, $C(x,y,z)=c$. If this intersection contains only one curve, then we choose initial conditions $(x_1,y_1,z_1)\in \mathcal{F}_{(h,c)}$. If the intersection contains more curves, then we compute initial conditions for one of these curves, using the condition $\mathcal{EC}(x_1,y_1,z_1)=(h,c)$. For example, if $(h,c)=(0,0.9)$ ($a=1$, $b=-1$), there are five orbits, as it is shown in Figure 8. We apply the mid-point rule (4.1) and at each step we impose the condition that the implicit solution is near the previous point (system (4.1) has not a unique solution). We implemented this algorithm in Wolfram Mathematica^{TM}. The code is given below.

$a=1; b=-1;\ \Delta t=0.03;\ k=1;\ kmax=400;\ x1=0.94868;\ y1=0.94868;\ z1=0;$
$\mathrm{Do}[v[k]=\{x1,y1,z1\};$
$s=\mathrm{NSolve}[$
$\frac{x-x1}{\Delta t}==a\frac{y1+y}{2}+\frac{b}{4}(y1+y)(z1+z)\&\&$
$\frac{y-y1}{\Delta t}==-a\frac{x1+x}{2}+\frac{b}{4}(x1+x)(z1+z)\&\&$
$\frac{z-z1}{\Delta t}==-\frac{(x1+x)(y1+y)}{4}\&\&$
$\mathrm{Norm}[x-x1]<2,\{x,y,z\},\mathrm{Reals}];$
$sx=s[[All,1,2]];\ sy=s[[All,2,2]];\ sz=s[[All,3,2]];$
$x1=sx[[1]],\ y1=sy[[1]],\ z1=sz[[1]],\ \{k,1,kmax\}];$
$data=\mathrm{Table}[v[k],\ \{k,1,kmax\}];$
$\mathrm{ListPointPlot3D}[data]$

The initial conditions given above lead to a periodic orbit (Figure 7). Moreover, if we choose other initial conditions, namely $x1=1.9748$, $y1=3.9874$, $z1=3$, $x1=-1.9748$, $y1=-3.9874$, $z1=3$, $x1=-3.9874$, $y1=1.9748$, $z1=-3$, and $x1=3.9874$, $y1=-1.9748$, $z1=-3$, other four orbits are obtained, respectively (see Figure 8).

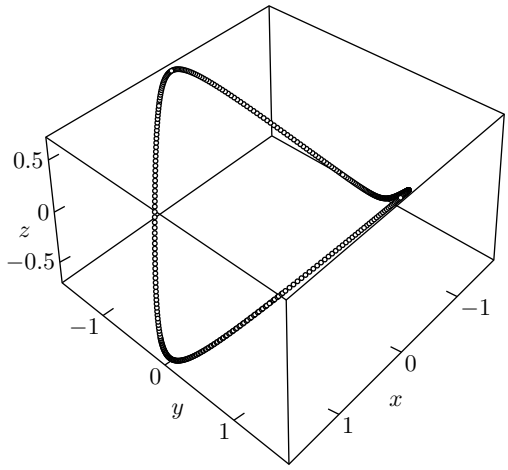

Figure 7. A periodic orbit $(h, c) = (0, 0.9)$, $a = 1, b = -1$, initial conditions $x_1 = 0.9487$, $y_1 = 0.9487, z_1 = 0$, the step $\Delta t = 0.03$.

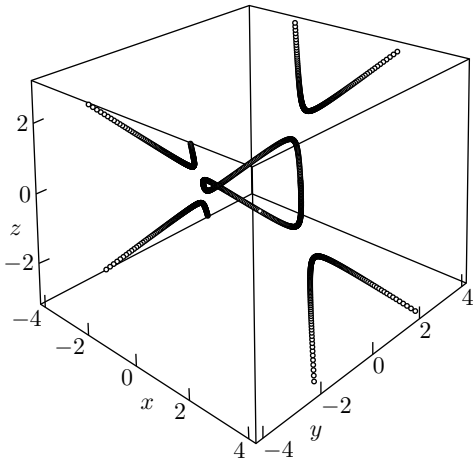

Figure 8. Numerical integration: 5 orbits at the intersection of the level sets $H(x, y, z) = h$, $C(x, y, z) = c$, $(h, c) = (0, 0.9)$, $a = 1$, $b = -1$.

In the same manner one can obtain any orbit. We highlight the pair of heteroclinic orbits shown in Figure 4. Consider $a = 1$, $b = -1$. Let $(h, c) \in \Sigma_1^u$ (3.12). We choose, for example, $h = -1$, $c = 0$. Fix $z_1 = -0.5$. We compute an initial point (x_1, y_1, z_1) that belongs to the intersection of the level sets $H(x, y, z) = -1$ and $C(x, y, z) = 0$. We obtain more points and we choose $(x_1, y_1, z_1) = (0.5, 0.5, -0.5)$. We again use the above-mentioned code and after 250 iterations ($\Delta t = 0.05$) one gets $(1.41421, 5.33122 \cdot 10^{-8}, -1)$, which is closer to the unstable equilibrium state $(M, 0, a/b) = (\sqrt{2}, 0, -1)$. Considering the same initial point and the time-step $\Delta t = -0.05$, we simulate the behavior of the orbit as $t \to -\infty$. After 250 iterations

we get $(-1.41421, 1.49088 \cdot 10^{-7}, -1)$, which is approximately the unstable equilibrium state $(-M, 0, a/b) = (-\sqrt{2}, 0, -1)$. Therefore, we have obtained a heteroclinic orbit. Analogously, we obtain the second heteroclinic orbit that connects the above equilibrium states. These orbits are plotted in Figure 9.

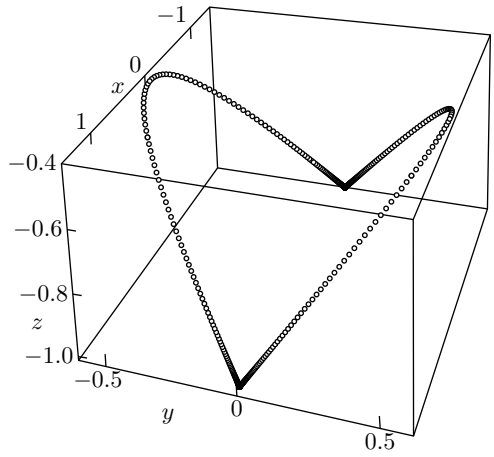

Figure 9. A pair of heteroclinic orbits for $(h, c) = (-1, 0)$, $a = 1$, $b = -1$.

5. Conclusion

In this paper we have considered an integrable deformation of an integrable version of the Rikitake system. The main goal is to analyze the changes in the dynamics of the initial system that appear by adding some parametric control functions such that the image of the corresponding energy-Casimir mapping is $\mathbb{R}^2$. The integrable version of the Rikitake system [38] has three families of equilibrium states. Two of those families contain only nonlinearly stable equilibrium states and around them there are periodic orbits. Moreover, each unstable equilibrium state that belongs to the third family is joined to itself by homoclinic orbits. On the other hand, the above-mentioned families of nonlinearly stable equilibrium states become families of unstable equilibrium states for the considered integrable deformation. In addition, heteroclinic orbits appear in its dynamics. Furthermore, we have noticed new types of orbits such as unbounded orbits, or some orbits that for $t \to \pm\infty$ behave like homoclinic or heteroclinic orbits, but they are split on two branches.

It is known that versions of the Rikitake two-disk dynamo system are chaotic for some values of the parameters (see, for example, [18]). It is natural to ask whether its particular deformation (2.9) considered in our paper also has chaotic behavior. Moreover, if deformation parameter b varies, does system (2.8) pass from a chaotic to

a non-chaotic state, or also can its unstable equilibrium states be stabilized? Taking into account that the above-mentioned system depends on many parameters, it can exhibit some types of bifurcations such as Hopf, zero-Hopf, Bogdanov-Takens, and Bautin bifurcations. These questions and many others can be the object of new papers.

References

[1] *R. M. Adams, R. Biggs, W. Holderbaum, C. C. Remsing*: On the stability and integration of Hamilton-Poisson systems on $\mathfrak{so}(3)^*_-$. Rend. Mat. Appl., VII. Ser. *37* (2016), 1–42. zbl MR

[2] *V. I. Arnol'd*: Conditions for nonlinear stability of stationary plane curvilinear flows on an ideal fluid. Sov. Math., Dokl. *6* (1965), 773–777; translation from Dokl. Akad. Nauk SSSR *162* (1965), 975–978. zbl MR doi

[3] *M. A. Austin, P. S. Krishnaprasad, L.-S. Wang*: Almost Poisson integration of rigid body systems. J. Comput. Phys. *107* (1993), 105–117. zbl MR doi

[4] *Á. Ballesteros, A. Blasco, F. Musso*: Integrable deformations of Rössler and Lorenz systems from Poisson-Lie groups. J. Differ. Equations *260* (2016), 8207–8228. zbl MR doi

[5] *D. I. Barrett, R. Biggs, C. C. Remsing*: Quadratic Hamilton-Poisson systems on $\mathfrak{se}(1,1)^*$: The inhomogeneous case. Acta Appl. Math. *154* (2018), 189–230. zbl MR doi

[6] *T. Bînzar, C. Lăzureanu*: A Rikitake type system with one control. Discrete Contin. Dyn. Syst, Ser. B. *18* (2013), 1755–1776. zbl MR doi

[7] *T. Bînzar, C. Lăzureanu*: On some dynamical and geometrical properties of the Maxwell-Bloch equations with a quadratic control. J. Geom. Phys. *70* (2013), 1–8. zbl MR doi

[8] *A. V. Bolsinov, A. V. Borisov*: Compatible Poisson brackets on Lie algebras. Math. Notes *72* (2002), 10–30; translation from Mat. Zametki *72* (2002), 11–34. zbl MR doi

[9] *D. R. J. Chillingworth, P. J. Holmes*: Dynamical systems and models for reversals of the earth's magnetic field. J. Internat. Assoc. Math. Geol. *12* (1980), 41–59. MR doi

[10] *A. E. Cook, P. H. Roberts*: The Rikitake two-disc dynamo system. Proc. Camb. Philos. Soc. *68* (1970), 547–569. doi

[11] *P. A. M. Dirac*: The Principles of Quantum Mechanics. Oxford University Press, Oxford, 1947. zbl MR

[12] *C. A. Evripidou, P. Kassotakis, P. Vanhaecke*: Integrable deformations of the Bogoyavlenskij-Itoh Lotka-Volterra systems. Regul. Chaotic Dyn. *22* (2017), 721–739. zbl MR doi

[13] *A. Galajinsky*: Remark on integrable deformations of the Euler top. J. Math. Anal. Appl. *416* (2014), 995–997. zbl MR doi

[14] *G. A. Glatzmaier, P. H. Roberts*: A three-dimensional self-consistent computer simulation of a geomagnetic field reversal. Nature *377* (1995), 203–209. doi

[15] *Y. Hardy, W.-H. Steeb*: The Rikitake two-disc dynamo system and domains with periodic orbits. Int. J. Theor. Phys. *38* (1999), 2413–2417. zbl MR doi

[16] *D. D. Holm, J. E. Marsden*: The rotor and the pendulum. Symplectic Geometry and Mathematical Physics. Birkhäuser, Boston, 1991, pp. 189–203. zbl MR doi

[17] *K. Huang, S. Shi, Z. Xu*: Integrable deformations, bi-Hamiltonian structures and non-integrability of a generalized Rikitake system. Int. J. Geom. Methods Mod. Phys. *16* (2019), Article ID 1950059, 17 pages. zbl MR doi

[18] *K. Ito*: Chaos in the Rikitake two-disc dynamo system. Earth Planet. Sci. Lett. *51* (1980), 451–456. doi

[19] *M. Ivan, G. Ivan*: On the fractional Euler top system with two parameters. Int. J. Modern Eng. Research *8* (2018), 10–22.

[20] *X. Jian*: Anti-synchronization of uncertain Rikitake systems via active sliding mode control. Int. J. Phys. Sci. *6* (2011), 2478–2482. doi
[21] *B. Kostant*: Quantization and unitary representations I. Prequantization. Lectures in Modern Analysis and Applications III. Lecture Notes in Mathematics 170. Springer, Berlin, 1970, pp. 87–208. zbl MR doi
[22] *C. Lăzureanu*: Hamilton-Poisson realizations of the integrable deformations of the Rikitake system. Adv. Math. Phys. *2017* (2017), Article ID 4596951, 9 pages. zbl MR doi
[23] *C. Lăzureanu*: On a Hamilton-Poisson approach of the Maxwell-Bloch equations with a control. Math. Phys. Anal. Geom. *20* (2017), Article ID 20, 22 pages. zbl MR doi
[24] *C. Lăzureanu*: On the Hamilton-Poisson realizations of the integrable deformations of the Maxwell-Bloch equations. C. R., Math., Acad. Sci. Paris *355* (2017), 596–600. zbl MR doi
[25] *C. Lăzureanu*: Integrable deformations of three-dimensional chaotic systems. Int. J. Bifurcation Chaos Appl. Sci. Eng. *28* (2018), Article ID 1850066, 7 pages. zbl MR doi
[26] *C. Lăzureanu, T. Bînzar*: A Rikitake type system with quadratic control. Int. J. Bifurcation Chaos Appl. Sci. Eng. *22* (2012), Article ID 1250274, 14 pages. zbl MR doi
[27] *C. Lăzureanu, T. Bînzar*: On the symmetries of a Rikitake type system. C. R., Math., Acad. Sci. Paris *350* (2012), 529–533. zbl MR doi
[28] *C. Lăzureanu, C. Petrişor*: Stability and energy-Casimir mapping for integrable deformations of the Kermack-McKendrick system. Adv. Math. Phys. *2018* (2018), Article ID 5398768, 9 pages. zbl MR doi
[29] *P. Libermann, C.-M. Marle*: Symplectic Geometry and Analytical Mechanics. Mathematics and Its Applications 35. D. Reidel, Dordrecht, 1987. zbl MR doi
[30] *J. Llibre, X. Zhang*: Invariant algebraic surfaces of the Rikitake system. J. Phys. A, Math. Gen. *33* (2000), 7613–7635. zbl MR doi
[31] *R. I. McLachlan*: On the numerical integration of ordinary differential equations by symmetric composition methods. SIAM J. Sci. Comput. *16* (1995), 151–168. zbl MR doi
[32] *T. McMillen*: The shape and dynamics of the Rikitake attractor. Nonlinear J. *1* (1999), 1–10.
[33] *J. Moser*: Periodic orbits near an equilibrium and a theorem by Alan Weinstein. Commun. Pure Appl. Math. *29* (1976), 727–747. zbl MR doi
[34] *I. Pehlivan, Y. Uyaroglu*: Rikitake attractor and it's synchronization application for secure communication systems. J. Appl. Sci. *7* (2007), 232–236. doi
[35] *M. Puta*: Hamiltonian Mechanical Systems and Geometric Quantization. Mathematics and Its Applications (Dordrecht) 260. Kluwer Academic, Dordrecht, 1993. zbl MR doi
[36] *M. Puta*: Lie-Trotter formula and Poisson dynamics. Int. J. Bifurcation Chaos Appl. Sci. Eng. *9* (1999), 555–559. zbl MR doi
[37] *T. Rikitake*: Oscillations of a system of disk dynamos. Proc. Camb. Philos. Soc. *54* (1958), 89–105. zbl MR doi
[38] *R. M. Tudoran, A. Aron, Ş. Nicoară*: On a Hamiltonian version of the Rikitake system. SIAM J. Appl. Dyn. Sys. *8* (2009), 454–479. zbl MR doi
[39] *R. M. Tudoran, A. Gîrban*: On a Hamiltonian version of a three-dimensional Lotka-Volterra system. Nonlinear Anal., Real World Appl. *13* (2012), 2304–2312. zbl MR doi
[40] *D. L. Turcotte*: Fractals and Chaos in Geology and Geophysics. Cambridge University Press, Cambridge, 1997. zbl MR doi
[41] *C. Valls*: Rikitake system: Analytic and Darbouxian integrals. Proc. R. Soc. Edinb., Sect. A, Math. *135* (2005), 1309–1326. zbl MR doi
[42] *V. Vembarasan P. Balasubramaniam*: Chaotic synchronization of Rikitake system based on T-S fuzzy control techniques. Nonlinear Dyn. *74* (2013), 31–44. zbl MR doi
[43] *U. E. Vincent*: Synchronization of Rikitake chaotic attractor using active control. Phys. Lett., A *343* (2005), 133–138. zbl doi

[44] *Z. Wei, W. Zhang, Z. Wang, M. Yao*: Hidden attractors and dynamical behaviors in an extended Rikitake system. Int. J. Bifurcation Chaos Appl. Sci. Eng. *25* (2015), Article ID 1550028, 11 pages. zbl MR doi

[45] *Z. Wei, B. Zhu, J. Yang, M. Perc, M. Slavinec*: Bifurcation analysis of two disc dynamos with viscous friction and multiple time delays. Appl. Math. Comput. *347* (2019), 265–281. zbl MR doi

Authors' address: *Cristian Lăzureanu* (corresponding author), *Camelia Petrişor*, *Ciprian Hedrea*, Department of Mathematics, Politehnica University of Timişoara, Piata Victoriei No. 2, 300006 Timişoara, Romania, e-mail: `cristian.lazureanu@upt.ro`, `camelia.petrisor@upt.ro`, `ciprian.hedrea@upt.ro`.